Electronic Supplementary Information

Reversible Two-channel Mechanochromic Luminescence for Pyridinium-based White-light Emitter with Room Temperature Fluorescence-Phosphorescence Dual Emission

Xiao Ma*, Jipeng Li , Chensheng Lin , Guoliang Chai, Yangbin Xie , Wei Huang , Dayu Wu* and Wai-Yeung Wong*

Materials and Methods

General Information. All of the chemicals were obtained from commercial sources and used without further purification. IR spectra were recorded in the range of 400-4000 cm^{-1} on a Nicolet (Impact 410) spectrometer with KBr pellets. The UV-Vis absorption spectra were measured with a Perkin Elmer Lambda 900 Spectrometer. Powder X-ray diffraction (PXRD) measurements were performed on a Bruker D8 Avance X-ray powder diffractometer with Cu Kα (1.5418 Å). NMR measurements were carried out on a Bruker DMX500 spectrometer using tetramethylsilane (TMS) as an internal standard. The elemental analysis was determined using a Vario EL III CHNOS elemental analyzer. Fluorescence spectra for the solid samples were recorded at room temperature on an Edinburgh Model FS5 instrument, and emission quantum yield were recorded on integrating sphere SC-30. Luminescence lifetimes (τ) were examined using an Edinburgh Model FLS920 phosphorimeter. The pressure-dependent emission spectra for **P1-PF$_6$** were measured by using infrared tablet press method.

X-ray Crystallography. Crystallographic data were collected on a Bruker Apex DUO CCD diffractometer with graphite-monochromated Mo Kα radiation (λ = 0.71073 Å) using the ω-scan technique. The intensity data were integrated by using the SAINT program.[1] An empirical absorption correction was applied using the SADABS program.[2] The structures were solved by direct method and the non-hydrogen atoms were located from the trial structures and then refined anisotropically with SHELXTL using full-matrix least-squares procedures based on F^2 values.[3] The positions of the non-hydrogen atoms were refined with anisotropic displacement factors.

Theoretical calculations

All calculations were performed using the Gaussian 09 series of programs.[4] The commonly used Becke's three parameter exchange functional combined with the LYP4 correlation functional (B3LYP) was used for the calculations. The geometry of **P1-PF$_6$** for calculations was taken from the X-ray diffraction data. The optimized excited-state geometries of **P1-PF$_6$** were calculated by time-dependent density functional theory (TD-DFT) at the B3LYP/6-31G(d) level.

Synthesis

2,6-Bis(4-bromophenyl)-4,4'-bipyridine (**L**): In a 250 mL round bottom flask, 1-(4-bromophenyl)ethanone (4.30 g, 21.6 mmol), NH_3 (aqueous) (15 mL) and KOH (2.3g, 41.0 mmol) were respectively added to a solution of 4-pyridinecarboxadehyde (1.14 g, 10.6 mmol) in EtOH (100 mL). The solution was refluxed for 24 h. After cooling down to the room temperature, the solution was evaporated to dryness under reduced pressure to give the crude product. The crude product was washed by cool methanol twice and then recrystallized by ethanol. A pure white solid was obtained. ^{1}H NMR: (400 MHz, DCM) δ 8.88 (2 H, s), 8.10 (4 H, d, *J* 8.0), 7.91 (2 H, s), 7.69 (6 H, d, *J* 12).

P1-Br: (Bromomethyl)benzene (0.073 g, 0.64 mmol) was added into a solution of **L** (0.3 g, 0.64 mmol) in CH_3CN (16 mL) and the reaction mixture was stirred at 90 °C under N_2 for 12 h. The resultant white precipitate was collected by filtration and washed with CH_3CN and DCM, giving the yellow product of **P1-Br** with the yield above 90%. ^{1}H NMR: (400 MHz, DMSO) δ 9.46 (2 H, d, *J* 8.0), 8.91 (2 H, d, *J* 8.0), 8.55 (2 H, s), 8.32 (2 H, d, *J* 8.0), 7.78 (4 H, d, *J* 8.0), 7.61 (2 H, d, *J* 4.0), 7.5-7.41 (3 H, m), 5.92 (2 H, s). IR (KBr, cm^{-1}): 3127(s) ,1635(w), 1542(w), 1401(s), 1155(w), 1070(m), 1005(m), 820(s), 743(m), 698(m), 617(m).

P1-PF$_6$: Excess NH_4PF_6 (100 mg) was added into a solution of **P1-Br** (150 mg) in CH_3OH (12 mL). The reaction mixture was stirred at room temperature for 12 h. The deposited light yellow microcrystals with the yield of ~90% were collected by filtration and washed with CH_3OH. The single crystal could be obtained from slow evaporation of acetonitrile and ethanol solution. Calcd. for C, 49.60; H, 3.01; N, 3.99; Found: C, 49.83; H, 2.99; N, 4.11; ^{1}H NMR: (400 MHz, DMSO) δ 9.45 (2 H, d, *J* 8.0), 8.90 (2 H, d, *J* 4.0), 8.55 (2 H, s), 8.32 (2 H, d, *J* 8.0), 7.78 (4 H, d, *J* 8.0), 7.59 (2 H, d, *J* 8.0), 7.50-7.42 (3 H, m), 5.90 (2 H, s). MS: m/z Calcd. for $C_{29}H_{21}Br_2F_6N_2P$: 557.00. IR (KBr, cm^{-1}): 3127(s) ,1671(m), 1643(m),1582(w), 1542(w), 1397(s), 1155(w), 1074(m), 1005(m), 832(s), 739(m), 698(m), 617(m), 557(m).

Table S1. Crystallographic data and a summary of the structural refinement results for P1-PF6

	P1-PF$_6$
formula	$C_{29}H_{21}N_2PF_6Br_2$
fw (g/mol)	702.27
color	light yellow
T (K)	175
Crystal system	monoclinic
Space group	*P 21/c*
Z	4
a [Å]	29.7525(17)
b [Å]	5.9838(3)
c [Å]	15.5910(7)
α [°]	90.00
β [°]	98.639(2)
γ [°]	90.00
V [Å^3]	2744.2(2)
Density (calcd.)[g·cm^{-3}]	1.700
μ [mm^{-1}]	3.076
θ-range [°]	2.77 to 25.38
Index range	$-34 \leq h \leq 35$
	$-7 \leq k \leq 7$
	$-18 \leq l \leq 18$
Reflections collected	15694
Unique reflections	5034
Observed reflections ($I > 2\sigma(I)$)	3685
parameters refined	361
Final R_1 values ($I > 2\sigma(I)$)	0.0448
Final w$R(F^2)$ values (I > 2σ(I))	0.1193
Final R_2 values (all data)	0.0746
Final w$R(F^2)$ values (all data)	0.1379
GOOF (goodness of fit)	0.907

$R_1 = \Sigma(||F_0| - |F_c||)/\Sigma|F_0|$;
$wR_2 = [\Sigma w(|F_0^2| - |F_c^2|)^2/\Sigma w|F_0^2|^2]^{1/2}$

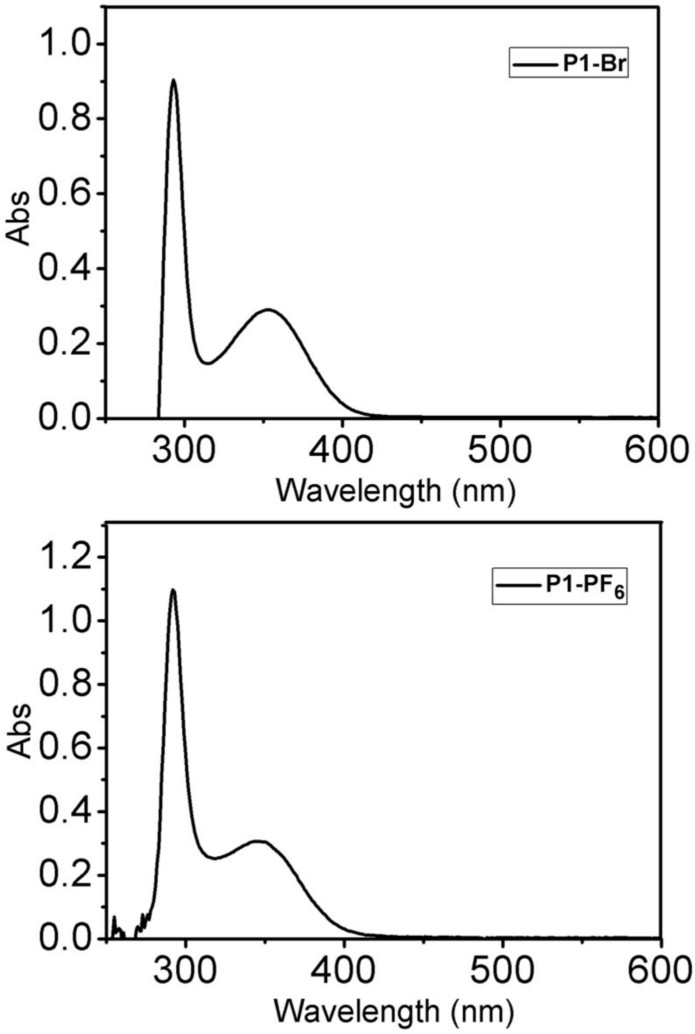

Fig. S1 UV-vis absorption spectra of both **P1-Br** (CH_3OH, 1.5x10^{-5} mol/L) and **P1-PF6** (CH_3CN, 2x10^{-5} mol/L).

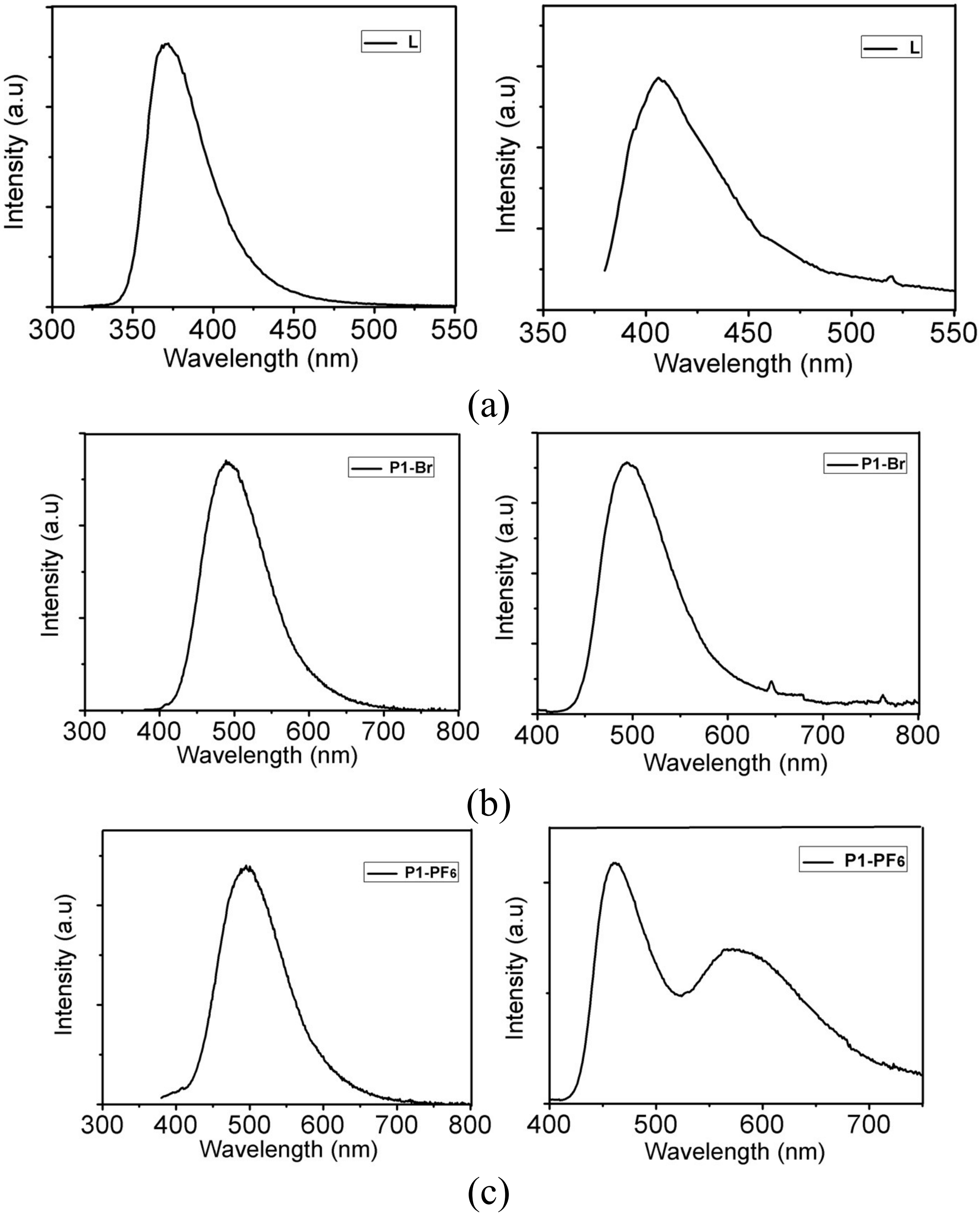

Fig. S2 Photoluminescence spectra of the compounds in solution and in solid state. a) **L** in DCM (2x10^{-5} mol/L, left) and in solid state (right); b) **P1-Br** in CH_3OH (1.5x10^{-5} mol/L, left) and in solid state (right); c) **P1-PF$_6$** in CH_3CN (2x10^{-5} mol/L, left) and in solid state (right).

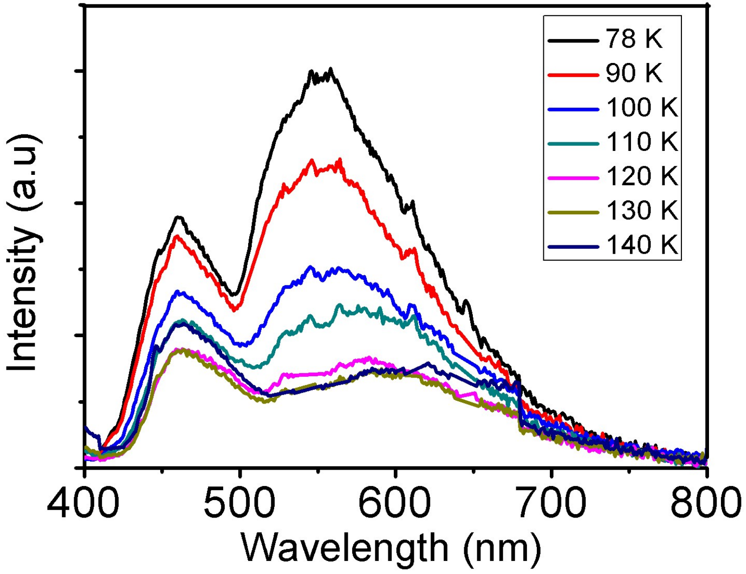

Fig. S3 The temperature-dependent emission spectra of **P1-PF$_6$** (λ_{ex} = 365 nm) from 140 K to 78 K.

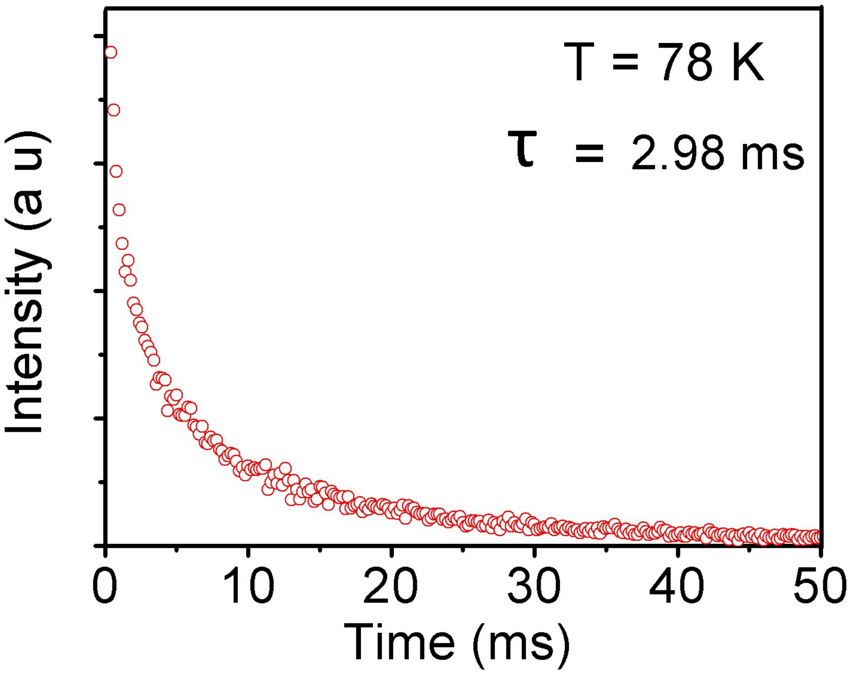

Fig. S4 Transient photoluminescence decay spectra of **P1-PF$_6$** for 582 nm at 78 K (λ_{ex} = 365 nm)

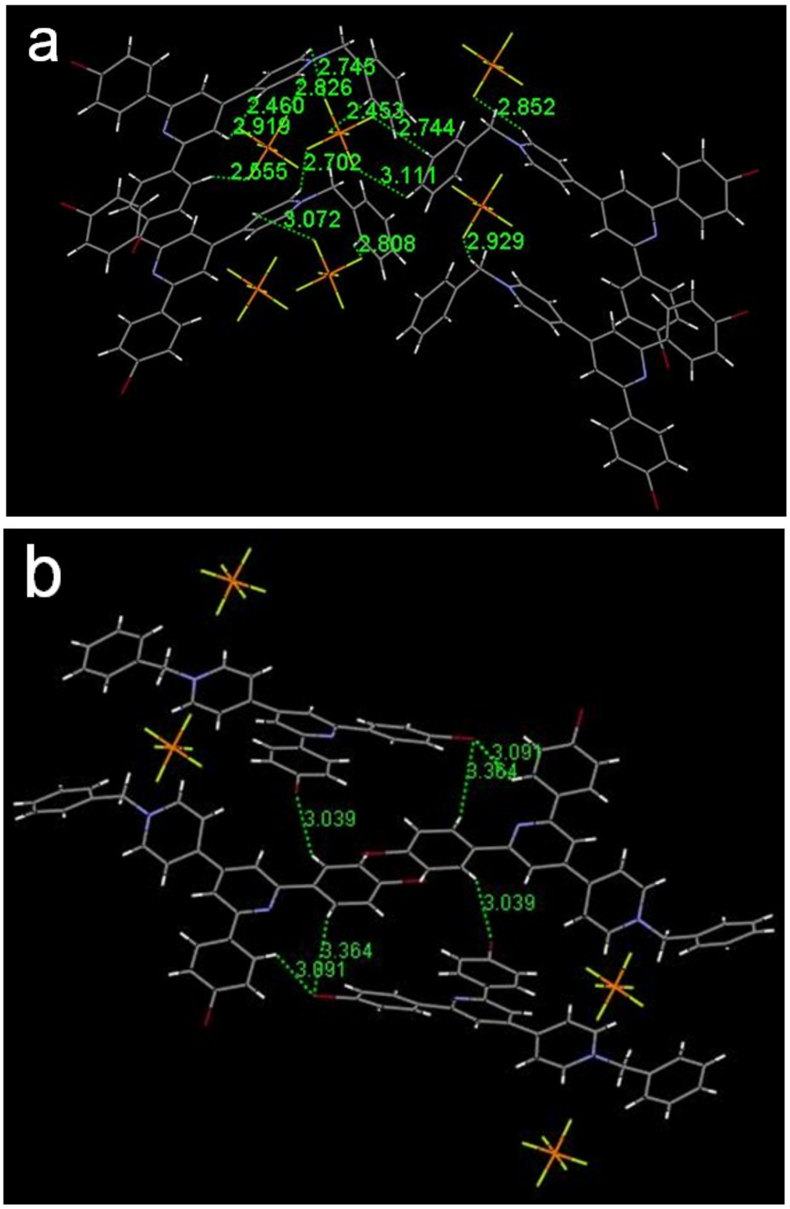

Fig. S5 Numerous C–H···F hydrogen bond interactions (a) and C–H···Br-C bond interactions (b) in the crystal **P1-PF$_6$**.

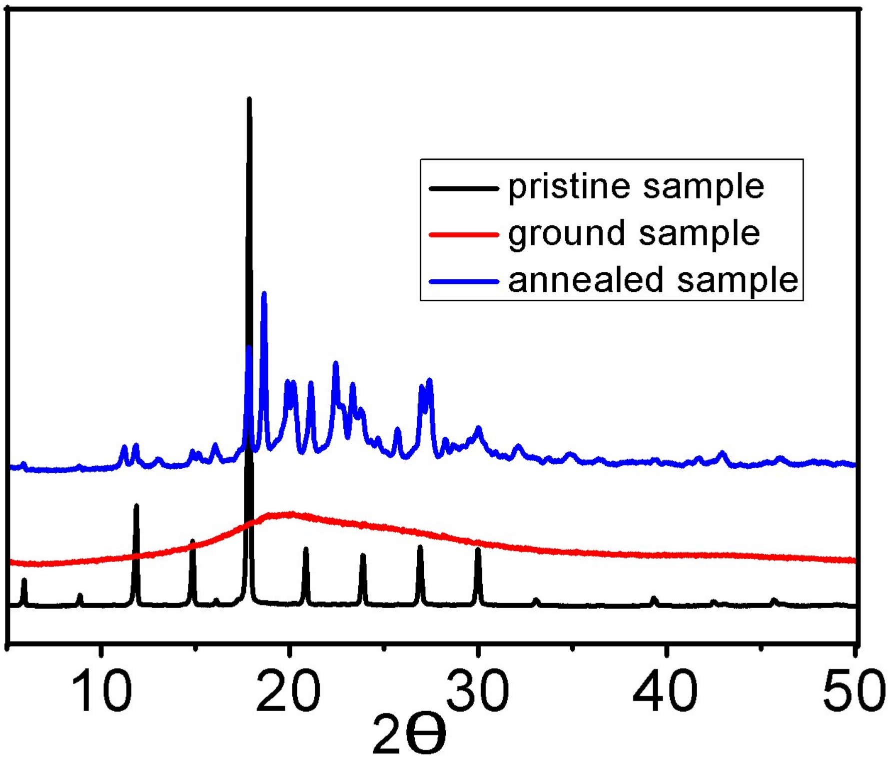

Fig. S6 X-ray powder diffractions of **P1-PF$_6$** for pristine sample (black), ground sample (red), annealed sample (blue)

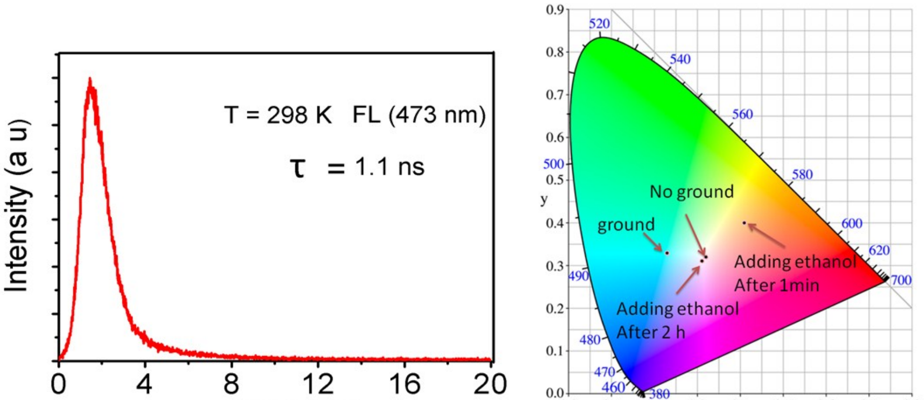

(a) (b)

Fig. S7 a) Transient photoluminescence decay spectra of **P1-PF$_6$** for 473 nm after heavy grinding at room temperature (λ_{ex} = 365 nm); b) The corresponding CIE chromaticity coordinates in CIE-1931 chromaticity diagram of **P1-PF$_6$** for the no **ground** samples, the **ground** samples, and the corresponding ground samples by adding ethanol after 1 min and after 2 h.

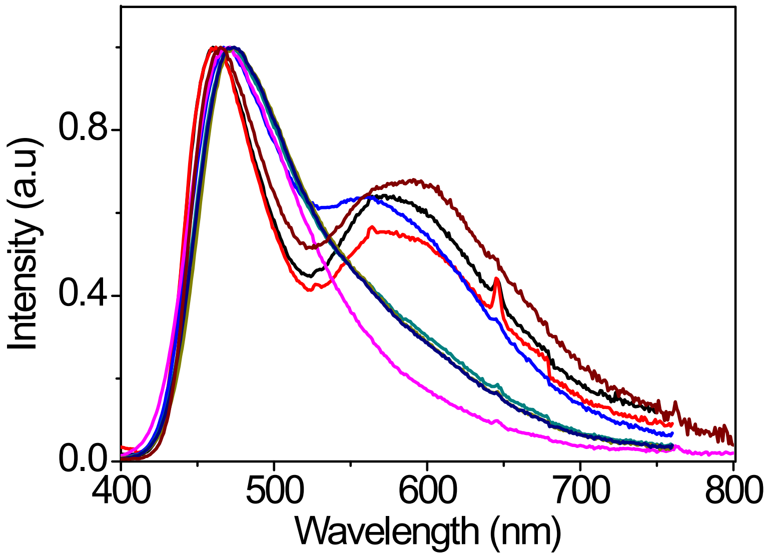

Fig. S8 Emission switching graphs of the **P1-PF$_6$** in multiple cycles upon the grinding/evaporation process.

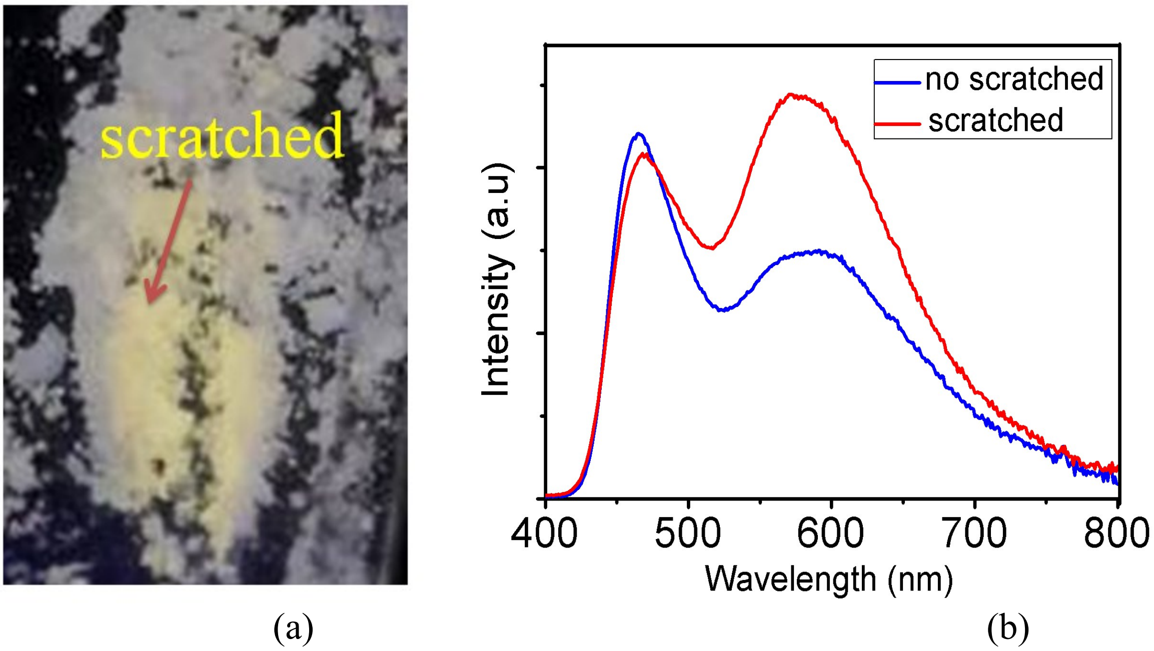

(a) (b)

Fig. S9 Emission photos of the **P1-PF$_6$** samples scratched by a steel scoop under 365 nm UV irradiation; b) The emission spectra of the scratched **P1-PF$_6$** (λ_{ex} = 365 nm)

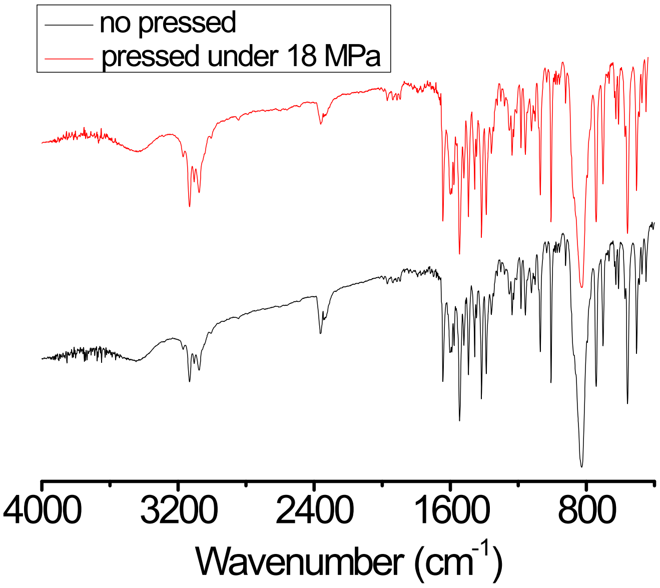

Fig. S10 IR spectra of **P1-PF$_6$** for the pressed samples and no pressed samples

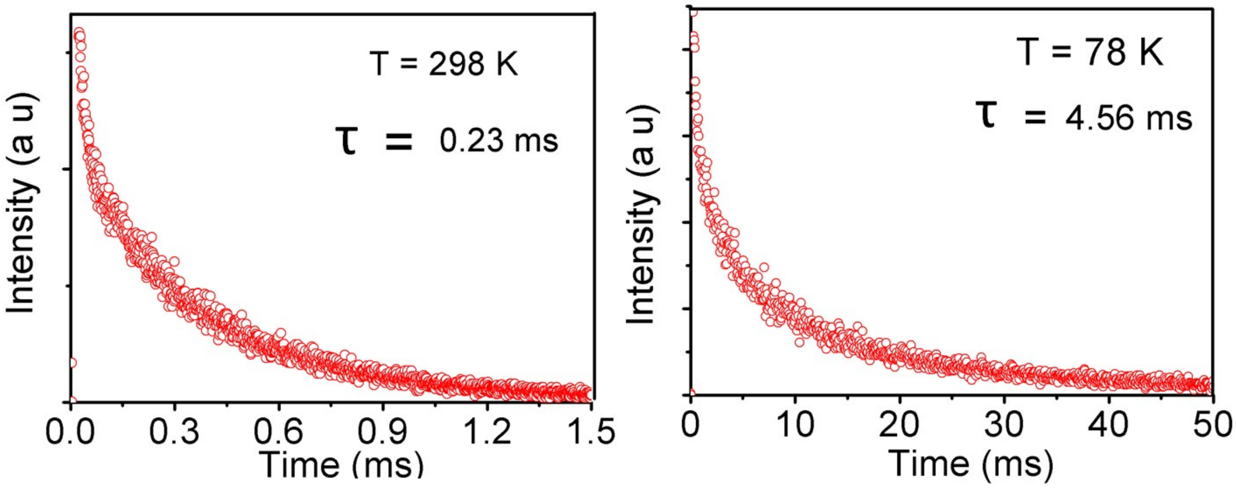

Fig. S11 Transient photoluminescence decay spectra of **P1-PF$_6$** for 582 nm (λ_{ex} = 365 nm) after mechanical pressing by using infrared tablet press method at room temperature and 78 K.

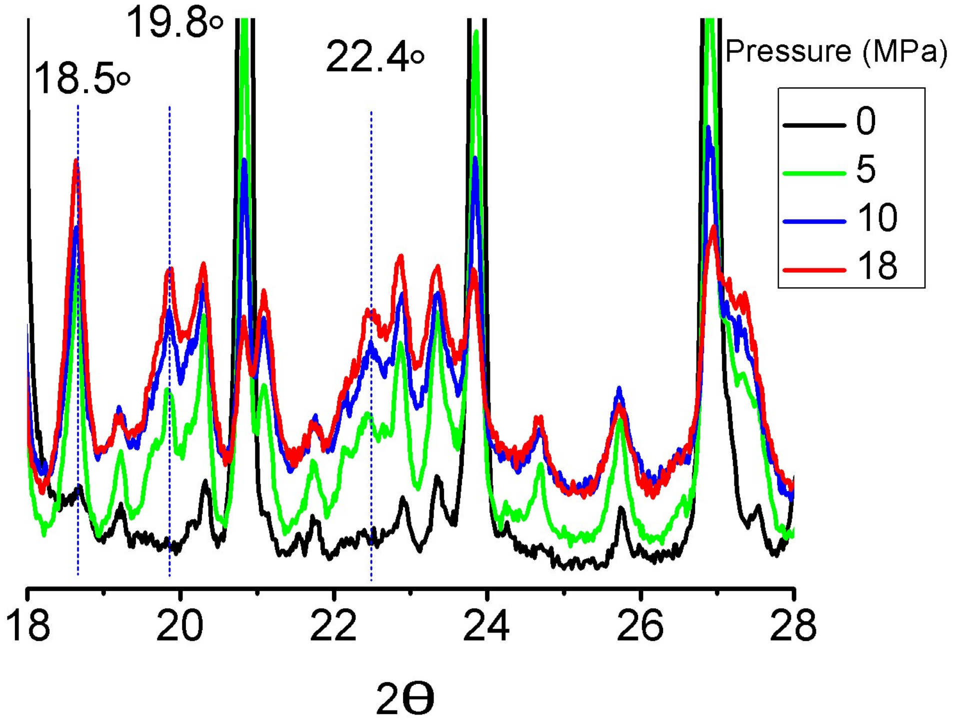

Fig. S12 X-ray powder diffractions of **P1-PF$_6$** under different pressures (2θ = 18° - 28°). After pressing, new peaks such as 2θ = 18.5°, 19.8° and 22.4° appear as compared to the original sample, and they rise in intensity gradually with increasing pressure.

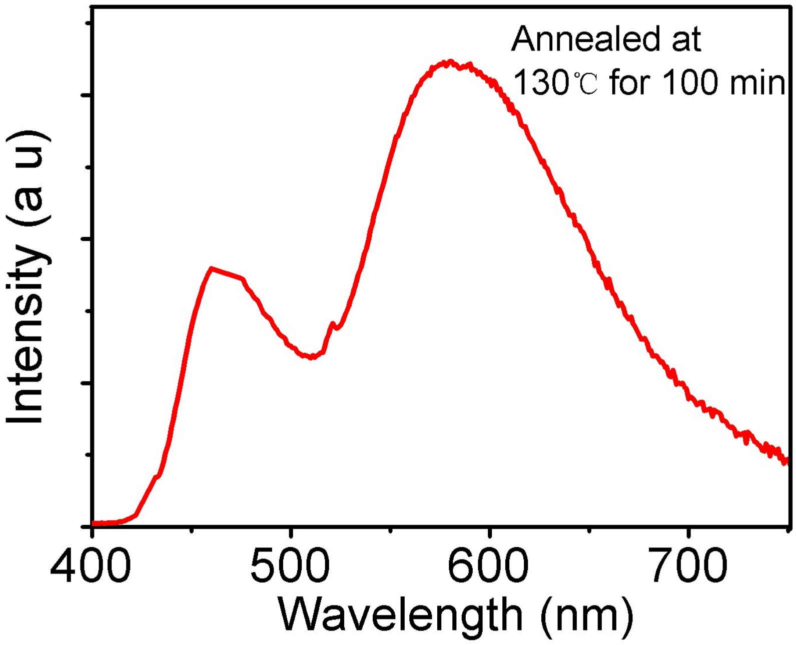

Fig. S13 The emission spectra of **P1-PF$_6$** (λ_{ex} = 365 nm) after heating at 130 °C for 100 min. The phosphorescent emission intensity of the pressed crystalline state **P1-PF$_6$** keeps almost unchanged

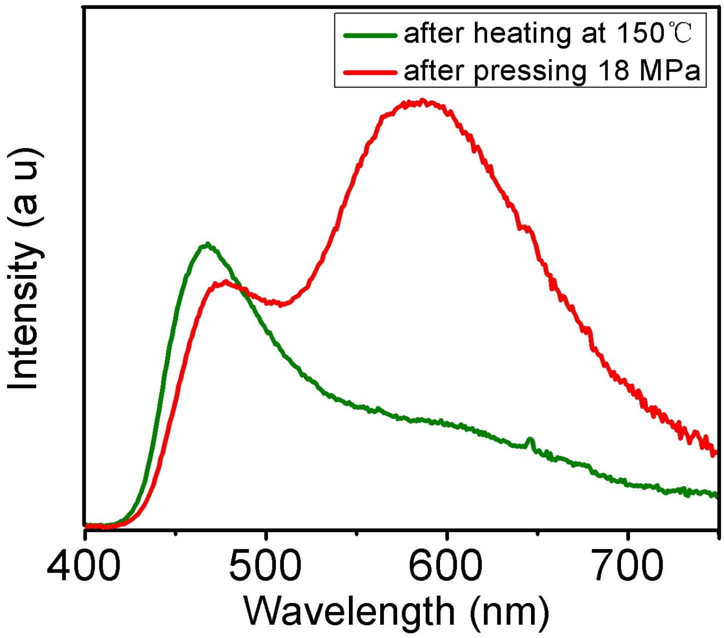

Fig. S14 The emission spectra of **P1-PF$_6$** (λ_{ex} = 365 nm) after heating at 150 °C for 20 min (green), and then repressing under 18 MPa (red) by using infrared tablet press method

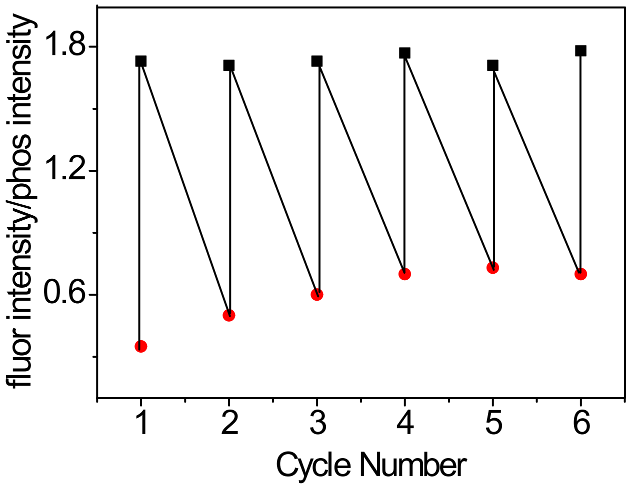

Fig. S15 The emission switching graph of **P1-PF$_6$** upon pressing-heating processes with fluor emission intensity/phos emission intensity vs cycle number

Table S2 The absorption transitions for dimer of **P1-PF$_6$** by TD-DFT method at the B3LYP/6-31G(d) level.

Orbital transition	Energy	f
346 → 349	1.05	0.000021
344 → 349	1.48	0.000202
342 → 349	1.58	0.000004
343 → 349	1.60	0.014454
341 → 349	1.62	0.000006
339 → 349	1.81	0.001782

References

[1] SMART & SAINT Software Reference Manuals, version 6.45; Bruker Analytical X-ray Systems, Inc.: Madison, WI, 2003.

[2] Sheldrick, G. M. SADABS: Software for Empirical Absorption Correction, version 2.05; University of Göttingen: Göttingen, Germany, 2002.

[3] Sheldrick, G. M. SHELXL97: Program for Crystal Structure Refinement; University of Göttingen: Göttingen, Germany, 1997.

[4] Gaussian 09, Revision A.02, Frisch, M. J.; Trucks, G. W.; Schlegel, H. B.; Scuseria, G. E.; Robb, M. A.; Cheeseman, J. R.; Scalmani, G.; Barone, V.; Mennucci, B.; Petersson, G. A.; Nakatsuji, H.; Caricato, M.; Li, X.; Hratchian, H. P.; Izmaylov, A. F.; Bloino, J.; Zheng, G.; Sonnenberg, J. L.; Hada, M.; Ehara, M.; Toyota, K.; Fukuda, R.; Hasegawa, J.; Ishida, M.; Nakajima, T.; Honda, Y.; Kitao, O.; Nakai, H.; Vreven, T.; Montgomery, J. A., Jr.; Peralta, J. E.; Ogliaro, F.; Bearpark, M.; Heyd, J. J.; Brothers, E.; Kudin, K. N.; Staroverov, V. N.; Kobayashi, R.; Normand, J.; Raghavachari, K.; Rendell, A.; Burant, J. C.; Iyengar, S. S.; Tomasi, J.; Cossi, M.; Rega, N.; Millam, J. M.; Klene, M.; Knox, J. E.; Cross, J. B.; Bakken, V.; Adamo, C.; Jaramillo, J.; Gomperts, R.; Stratmann, R. E.; Yazyev, O.; Austin, A. J.; Cammi, R.; Pomelli, C.; Ochterski, J. W.; Martin, R. L.; Morokuma, K.; Zakrzewski, V. G.; Voth, G. A.; Salvador, P.; Dannenberg, J. J.; Dapprich, S.; Daniels, A. D.; Farkas, O.; Foresman, J. B.; Ortiz, J. V.;Cioslowski, J.; Fox, D. J. Gaussian, Inc., Wallingford CT, 2009.